

буждения ЭЛ, оценить величину напряжения пробоя исследуемого образца.

Установка была апробирована на структурах Si/SiO<sub>2</sub>, Si/SiO<sub>2</sub>/Si<sub>3</sub>N<sub>4</sub>, Si/SiO<sub>2</sub>/SiN<sub>x</sub>/SiO<sub>2</sub>. На рисунке 3 представлены спектры ЭЛ образцов Si/SiO<sub>2</sub>/SiN<sub>0,9</sub>/SiO<sub>2</sub>, зарегистрированные при различных плотностях протекающего тока. Диэлектрические слои оксида и нитрида кремния сформированы методом химического осаждения из газовой фазы на кремниевой пластине p-типа. Общая толщина диэлектрических слоев составляет 140 нм. Спектры ЭЛ зарегистрированы при анодной поляризации кремниевой подложки.

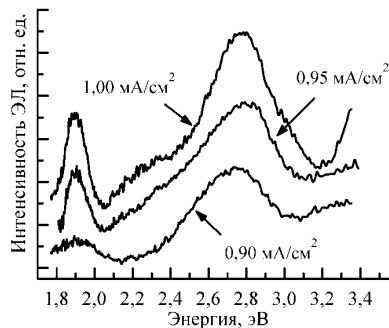


Рисунок 3 – Спектры электролюминесценции образца p-Si/SiO<sub>2</sub>/SiN<sub>0,9</sub>/SiO<sub>2</sub>

Спектры ЭЛ характеризуются полосами с энергиями в красной (1,9 эВ), зеленой (2,3 эВ) и синей (2,7 эВ) области, причем последняя полоса имеет наибольшую интенсивность. Полоса

в красной области спектра ЭЛ связана с наличием в слоях SiO<sub>2</sub> силанольных групп (Si-OH). ЭЛ в зеленой области объясняется внутрицентровыми переходами в атомах трехкоординированного кремния в слоях SiO<sub>2</sub>. Интенсивная полоса ЭЛ с максимумом при 2,7 эВ характерна для излучательной релаксации силиленовых центров [2]. Наличие этих центров присуще слоям оксинитрида кремния, что позволило сделать заключение о формировании таких слоев на границах оксида и нитрида кремния. Установлено, что интенсивность свечения этой полосы обладает наибольшей устойчивостью к воздействию сильных электрических полей после протекания через образец заряда 1-3 Кл/см<sup>2</sup>.

Таким образом, реализованный метод электролюминесценции позволяет изучить состав, структурные особенности, определить концентрацию центров люминесценции, исследовать деградацию диэлектрических слоев в результате воздействия сильного электрического поля.

### Литература

- Барабан, А.П. Электроника слоев SiO<sub>2</sub> на кремнии / А.П. Барабан, В.В. Булавинов, П.П. Коноров. – Л. : Изд. ЛГУ, 1988. – 304 с.
- Baraban, A.P. Electroluminescence of Si-SiO<sub>2</sub>-Si<sub>3</sub>N<sub>4</sub> structures / A.P. Baraban [et al.] // Technical Physics Letters. – 2002. – Vol. 28, № 12. – P. 978–980.

UDC 621

## ANISOTROPY OF THERMO-OPTICAL COEFFICIENTS OF ALEXANDRITE LASER CRYSTAL

P. Loiko<sup>1</sup>, S. Ghanbari<sup>2</sup>, V. Matrosov<sup>3</sup>, K. Yumashev<sup>4</sup>, A. Major<sup>2</sup>

<sup>1</sup> ITMO University, Saint-Petersburg, Russia

<sup>2</sup> Department of Electrical and Computer Engineering, University of Manitoba, Winnipeg, Canada

<sup>3</sup> Solix Ltd., Minsk, Belarus

<sup>4</sup> Center for Optical Materials and Technologies, Belarusian National Technical University, Minsk, Belarus

Alexandrite (Cr<sup>3+</sup>:BeAl<sub>2</sub>O<sub>4</sub>) is a well-known crystal for tunable lasers relying on vibronic coupling [1–3]. Alexandrite provides intense emission between 0.7 and 0.85 μm with a maximum at around 0.75 μm [4, 5]. The corresponding stimulated-emission cross-section is relatively small,  $\sigma_{SE} = 0.7 \times 10^{-20} \text{ cm}^2$ , which is compensated by a relatively long lifetime of the upper laser level  $\tau \sim 260 \mu\text{s}$  at room temperature. Thus, the ( $\sigma_{SET}$ ) product is large and the efficient and low-threshold continuous-wave laser operation of alexandrite is possible [6]. The Cr<sup>3+</sup> ions in orthorhombic BeAl<sub>2</sub>O<sub>4</sub> exhibit strong polarization-anisotropy of the spectroscopic properties (the high-gain light polarization is  $E \parallel b$ ) [4, 5] and linearly polarized laser output is easily achievable.

The Alexandrite lasers have relevant applications in medicine (dermatology), space LIDAR technologies, spectroscopy [7] and can replace Ti:Sapphire lasers in nonlinear microscopy.

Alexandrite exhibits a combination of attractive thermal and mechanical properties, namely very high thermal conductivity  $\kappa \sim 23 \text{ W/(mK)}$ , weak and almost isotropic thermal expansion  $\alpha \sim 7 \times 10^{-6} \text{ K}^{-1}$ , and high optical damage threshold [3, 8]. However, thermo-optical properties of alexandrite have not been studied in detail to date.

In the present report, we aimed to measure the thermo-optic coefficients (TOCs,  $dn/dT$ ) and to characterize thermal variation of the optical path length of alexandrite with respect to light polarization.

Alexandrite is orthorhombic (sp. gr. *Pnma*) and thus optically biaxial [9]. Its optical properties are characterized in the frame of the optical indicatrix. The optical indicatrix axes are mutually orthogonal and they coincide with the crystallographic axes *a*, *b*, *c*. The corresponding principal refractive indices are  $n_a$ ,  $n_b$  and  $n_c$  (for polarizations  $E \parallel a$ ,  $E \parallel b$  and  $E \parallel c$ , respectively) with  $n_c < n_a < n_b$ . Similarly to the

refractive indices, three principal TOCs exist for alexandrite, namely  $dn_a/dT$ ,  $dn_b/dT$  and  $dn_c/dT$ . No predefined relation for the corresponding TOCs is expected.

For the measurements of TOCs of alexandrite, the laser beam deviation method for a material with a linear thermal gradient was used [10]. The measurements were done using a 0.06 at.% Cr<sup>3+</sup>:BeAl<sub>2</sub>O<sub>4</sub> crystal (Solix Ltd.) which was cut to a rectangular sample with dimensions of 5.58(a) × 6.22(b) × 6.87(c) mm<sup>3</sup>. All six surfaces were polished to a laser grade quality. A set of probe lasers emitting in the spectral range of 0.4–1.1 μm was used. The probe radiation was linearly polarized. The measurements were done at 298 K. The linear temperature gradient in the sample was ~1–2 K/mm. It was determined separately for each sample orientation. The actual temperature of the hot and cold surfaces of the crystal was measured using sensitive thermocouples with a precision of 0.1 K.

The laser beam deviation method allows one to measure the so-called thermal coefficients of the optical path (TCOP),  $dn/dT + (n - 1)\alpha$ . The precision of the TCOP measurements was 7–10% depending on the crystal cut. The  $n$  and  $dn/dT$  are determined by light polarization  $E$  and  $\alpha$  (the linear thermal expansion coefficient) is determined by light propagation direction  $k$ . For orthorhombic Alexandrite, there are three principal  $\alpha$  values along the **a**, **b** and **c** directions ( $\alpha_a$ ,  $\alpha_b$  and  $\alpha_c$ , respectively). For any biaxial crystal incl. alexandrite, a total of 6 independent TCOPs can be measured leading to 3 principal TOCs each of which is determined from two measurements [10].

At first, we measured the six principal thermal coefficients of the optical path (TCOPs). Their dispersion is illustrated in Fig. 1 (a–c). All TCOPs are positive in the whole studied spectral range. The TCOP values show a polarization-anisotropy which is especially clear for the **a**-cut and **b**-cut crystals. In order to calculate the TOCs, i.e.,  $dn/dT = TCOP - (n - 1)\alpha$ , we used the literature data on the refractive index (calculated from the Sellmeier equations reported in [16]) and on the linear thermal expansion coefficients ( $\alpha_a = 5.9$ ,  $\alpha_b = 6.1$ ,  $\alpha_c = 6.7 \times 10^{-6}$  K<sup>−1</sup> [3, 7]). The results are shown in Fig. 1 (d). All three principal TOCs for alexandrite are positive and show a notable anisotropy. For the whole studied spectral range,  $dn_c/dT > dn_b/dT > dn_a/dT$ . The TOCs determined from the measurements for different crystal cut were in good agreement with each other, as indicated by the error bars in Fig. 1 (d).

To calculate the TCOPs and  $dn/dT$  at the particular laser wavelength, the dispersion of the  $dn/dT$  was modeled taking into account (i) volumetric thermal expansion (expressed by the  $\alpha_{vol} = \alpha_a + \alpha_b + \alpha_c$  coefficient) and (ii) temperature dependence of the electronic bandgap  $E_g$  (expressed by a temperature derivative,  $dE_g/dT$ ) [10]:

$$dn_i/dT = -\alpha_{vol} \frac{(n_\infty - 1)}{2n_i(\lambda)} \frac{\lambda^2}{\lambda^2 - \lambda_{ig}^2} - \frac{1}{E_{ig}} \frac{dE_{ig}}{dT} \frac{(n_\infty - 1)}{2n_i(\lambda)} \left( \frac{\lambda^2}{\lambda^2 - \lambda_{ig}^2} \right)^2. \quad (1)$$

In the Eq. (1),  $i = a, b, c$ ,  $\lambda$  is the light wavelength;  $\lambda_g$  [μm] = 1.2398/E<sub>g</sub> [eV],  $n(\lambda)$  is the Sellmeier equation,  $n_\infty$  is the refractive index in the long-wavelength infrared limit, see Ref [9]. The  $dn/dT$  value can be represented as a sum of two terms related to (i) and (ii) effects,  $(dn/dT)_a + (dn/dT)_g$ , which have negative and positive values, respectively. The experimental data in Fig. 1 (d) were modeled with Eq. (1) with  $E_g$  and  $dE_g/dT$  as free parameters leading to the thermo-optic dispersion curves. The best-fit parameters, depending on the light polarization, are in the range of 5.7–6.3 eV and  $-1.4 - 2.7 \times 10^{-4}$  eV/K, respectively. For alexandrite, the density functional theory predicts a direct bandgap of 6.45 eV [11] while the UV absorption edge is located at about 9 eV [3]. According to the Eq. (1), the positive  $dn/dT$  coefficients of alexandrite are related to the weak thermal expansion, so that the contribution of the  $(dn/dT)_g$  term is dominant.

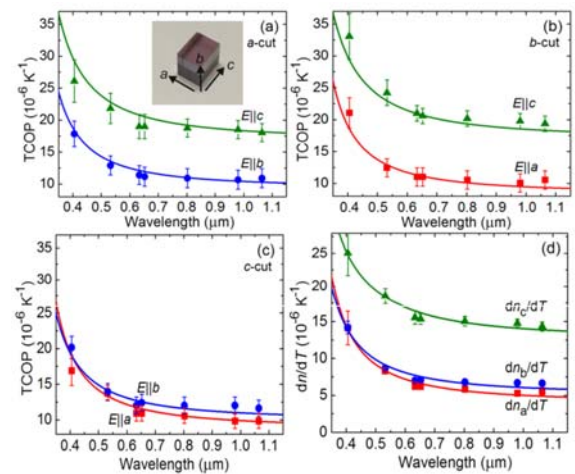


Fig. 1. Thermo-optical properties of alexandrite: (a–c) dispersion of TCOP for the **a**-cut (a), **b**-cut (b) and **c**-cut (c) crystals: symbols – experimental data, curves – data calculated using the thermo-optic dispersion formulas, Eq. (2), error bars indicate the uncertainty arising from the laser beam deviation method; (d) dispersion of TOCs: symbols – experimental data, curves – their fitting with Eq. (1), error bars indicate the uncertainty arising from the averaging of the  $dn/dT$  values for two different crystal cuts. Inset in (a) – photo of the studied crystal

The thermo-optic dispersion formulas can be also represented in a simplified form [10]:

$$dn/dT = A_0 + \frac{A_1}{\lambda^2} + \frac{A_2}{\lambda^4} + \frac{A_3}{\lambda^6}, \quad 10^{-6} K^{-1}. \quad (2)$$

Here,  $\lambda$  is in μm;  $A_{0-3}$  are the expansion coefficients ( $A_0$  corresponds to the  $dn/dT$  value in the long-wavelength limit,  $A_{1-3}$  represent its dispersion), see Table 1.

Using the derived thermo-optic dispersion formulas, we calculated TOCs at 0.75  $\mu\text{m}$  as  $dn_a/dT = 5.9$ ,  $dn_b/dT = 6.9$  and  $dn_c/dT = 15.2 \times 10^{-6} \text{ K}^{-1}$ . The anisotropy of the  $dn/dT$  values is much stronger than that of the refractive indices,  $n_a = 1.737$ ,  $n_b = 1.742$ ,  $n_c = 1.735$  at 0.75  $\mu\text{m}$  [9]. The values of the  $dn_a/dT$  and  $dn_b/dT$  are lower than 9.4 and  $8.3 \times 10^{-6} \text{ K}^{-1}$ , respectively, previously measured at 1150 nm [2]. There is no previous data on the  $dn^c/dT$ . Furthermore, we calculated the dispersion curves for the TCOP values,  $\text{TCOP}(\lambda) = dn/dT(\lambda) + [n(\lambda) - 1]\alpha$ , see Fig. 1 (a-c). The six principal TCOPs at 0.75  $\mu\text{m}$  are listed in Table 2. In particular, for a *c*-cut crystal and light polarization  $E \parallel b$ ,  $\text{TCOP} = 11.9 \times 10^{-6} \text{ K}^{-1}$ .

Table 1. Coefficients in the Thermo-Optic Dispersion Formulas for Alexandrite Crystal, Eq. (2)

| TOC       | $A_0$ | $A_1, \mu\text{m}^2$ | $A_2, \mu\text{m}^4$ | $A_3, \mu\text{m}^6$ |
|-----------|-------|----------------------|----------------------|----------------------|
| $dn_a/dT$ | 3.95  | 1.1842               | 0.0786               | 0.0246               |
| $dn_b/dT$ | 5.12  | 0.9848               | 0.0129               | 0.0141               |
| $dn_c/dT$ | 12.72 | 1.3275               | 0.0320               | 0.0121               |

Table 2. Thermal coefficients of the optical path ( $10^{-6} \text{ K}^{-1}$ ) of alexandrite crystal at 0.75  $\mu\text{m}$

| Crystal cut   | Polarization    |                 |                 |
|---------------|-----------------|-----------------|-----------------|
|               | $E \parallel a$ | $E \parallel b$ | $E \parallel c$ |
| <i>a</i> -cut | –               | +11.2           | +19.5           |
| <i>b</i> -cut | +10.4           | –               | +19.7           |
| <i>c</i> -cut | +10.8           | +11.9           | –               |

To conclude, we have studied dispersion and anisotropy of the  $dn/dT$  coefficients and TCOPs of alexandrite laser crystal. All three principal  $dn/dT$  are positive (due to the dominant effect of temperature variation of the bandgap over the weak thermal expansion) and they exhibit a notable polarization-anisotropy,  $dn_c/dT > dn_b/dT > dn_a/dT$ . For the high-gain laser polarization ( $E \parallel b$ ),  $dn/dT$  has an intermediate value of  $6.9 \times 10^{-6} \text{ K}^{-1}$  at 0.75  $\mu\text{m}$ . Positive  $dn/dT$  underlies positive (focusing) thermal lens of alexandrite lasers. We believe that a detailed knowledge of the thermo-optical properties of alexandrite crystal will help in designing laser cavities of high-power oscillators based on this laser crystal.

## References

1. J.C. Walling, O.G. Peterson, H.P. Jenssen, R.C. Morris, and E.W. O'Dell, «Tunable Alexandrite lasers», IEEE J. Quantum Electron. 16(12), 1302–1315 (1980).
2. J. Walling, F.H. Donald, H. Samelson, D.J. Harter, J. Pete, and R. C. Morris, «Tunable Alexandrite lasers: development and performance», IEEE J. Quantum Electron. 21(10), 1568–1581 (1985).
3. C.F. Cline, R.C. Morris, M. Dutoit, and P.J. Harget, «Physical properties of BeAl<sub>2</sub>O<sub>4</sub> single crystals», J. Mater. Sci. 14(4), 941–944 (1979).
4. R.C. Powell, L. Xi, X. Gang, G.J. Quarles, and J.C. Walling, «Spectroscopic properties of alexandrite crystals», Phys. Rev. B Condens. Matter 32(5), 2788–2797 (1985).
5. E.V. Pestryakov, A.I. Alimiev, and V.N. Matrosov, «Prospects for the development of femtosecond laser systems based on beryllium aluminate crystals doped with chromium and titanium ions», Quantum Electron. 31(8), 689–696 (2001).
6. S. Ghanbari and A. Major, «High power continuous-wave Alexandrite laser with green pump», Laser Phys. 26(7), 075001 (2016).
7. H. Samelson, J.C. Walling, and D.F. Heller, «Unique applications of alexandrite lasers», Proc. SPIE 0335, 85–94 (1983).
8. D.A. Vinnik, P.A. Popov, S.A. Archugov, and G.G. Mikhailov, «Heat conductivity of chromium-doped alexandrite single crystals», Dokl. Phys. 54(10), 449–450 (2009).
9. P. Loiko and A. Major, «Dispersive properties of alexandrite and beryllium hexaaluminate crystals», Opt. Mater. Express 6(7), 2177–2183 (2016).
10. P.A. Loiko, K.V. Yumashev, N.V. Kuleshov, G.E. Rachkovskaya and A.A. Pavlyuk, «Thermo-optic dispersion formulas for monoclinic double tungstates KRe(WO<sub>4</sub>)<sub>2</sub> where Re = Gd, Y, Lu, Yb», Opt. Mater. 33(11), 1688–1694 (2011).
11. W.Y. Ching, Y.-N. Xu, and B.K. Brickeen, «Comparative study of the electronic structure of two laser crystals: BeAl<sub>2</sub>O<sub>4</sub> and LiYF<sub>4</sub>», Phys. Rev. B 63(11), 115101 (2001).

УДК 535-7

## ОПРЕДЕЛЕНИЕ ПОКАЗАТЕЛЯ ПРЕЛОМЛЕНИЯ БИОЛОГИЧЕСКИХ МУТНЫХ СРЕД МЕТОДАМИ ЭЛЛИПСОИДАЛЬНЫХ РЕФЛЕКТОРОВ

Маяренко Д.Ю., Безуглая Н.В.

Национальный технический университет Украины  
«Киевский политехнический институт имени Игоря Сикорского», Киев, Украина

В основе методов исследования показателя преломления биологических сред лежат три основных физических явления: рефракция, интерференция и полное внутреннее отражение (ПВО). Измерительные средства могут быть реализованы как на одном явлении, так и нескольких [1]. Наиболее распространеными можно считать методы технической реализации, бази-

рующиеся на измерении критического угла (полного внутреннего отражения) в отраженном от объекта свете [2–6]. В общем случае они дают высокую точность, но, анализируя применение этих методов относительно мутных биологических сред и полученные с их помощью результаты, можно сделать вывод, что значения показателя преломления для одинаковых биологиче-